LETTERS

Towards molecular electronics with large-area molecular junctions

Hylke B. Akkerman[1], Paul W. M. Blom[1], Dago M. de Leeuw[2] & Bert de Boer[1]

Electronic transport through single molecules has been studied extensively by academic[1–8] and industrial[9,10] research groups. Discrete tunnel junctions, or molecular diodes, have been reported using scanning probes[11,12], break junctions[13,14], metallic crossbars[6] and nanopores[8,15]. For technological applications, molecular tunnel junctions must be reliable, stable and reproducible. The conductance per molecule, however, typically varies by many orders of magnitude[5]. Self-assembled monolayers (SAMs) may offer a promising route to the fabrication of reliable devices, and charge transport through SAMs of alkanethiols within nanopores is well understood, with non-resonant tunnelling dominating the transport mechanism[8]. Unfortunately, electrical shorts in SAMs are often formed upon vapour deposition of the top electrode[16–18], which limits the diameter of the nanopore diodes to about 45 nm. Here we demonstrate a method to manufacture molecular junctions with diameters up to 100 μm with high yields (>95 per cent). The junctions show excellent stability and reproducibility, and the conductance per unit area is similar to that obtained for benchmark nanopore diodes. Our technique involves processing the molecular junctions in the holes of a lithographically patterned photoresist, and then inserting a conducting polymer interlayer between the SAM and the metal top electrode. This simple approach is potentially low-cost and could pave the way for practical molecular electronics.

The theoretical prediction of unipolar molecular diodes[4] has led to a global effort to experimentally verify such devices. The envisaged application is molecular electronics, which could potentially solve fundamental scaling limits in complementary metal oxide semiconductor (CMOS) integrated circuits. Electronic transport in single molecules has been investigated with break junctions and a variety of scanning probe techniques. The conductance per molecule, however, differs by orders of magnitude. This discrepancy is probably due to the presence of an additional tunnelling gap in scanning probe techniques, to uncertainties in the number of molecules measured, or to poorly defined device surface areas (ref. 5 and references therein). Well-defined junctions can only be realized when the molecules are sandwiched between two electrodes. To ensure that electrical transport is dominated by the molecules and will therefore scale with the device area, an ordered monolayer is required. Typically, SAMs of alkanethiols on noble metals such as gold are used (ref. 19, and ref. 20 and references therein). Densely packed mono-domains of up to several hundred square nanometres can easily be formed when the chain length exceeds ten units (ref. 20 and references therein, and ref. 21).

Metal/SAM/metal nanojunctions about 45 nm in diameter have been fabricated using electron beam lithography and suspended silicon nitride membranes[8]. The conductance through the SAM of alkane thiols in the nanopores is independent of temperature and exponentially dependent on the length of the molecule[8], which implies that the electrical transport mechanism is non-resonant through-bond tunnelling. Therefore, the conductance per unit area through a SAM of alkane(di)thiols can be considered a benchmark for any novel technology related to molecular electronics.

The critical step in the fabrication of molecular junctions is applying the metal top electrode. Vapour-deposited noble metals create shorts in the SAMs due to filamentary growth[16–18], while reactive metals such as Ti destroy the SAM[16,18,22]. Here we report a technology that overcomes this difficulty and produces reliable, stable and reproducible molecular junctions. We prevent shorts by using a layer of highly conducting polymer between the SAM and the vapour-deposited metal top electrode. The molecular junctions are processed in vertical interconnects (or via holes) of photolithographically patterned photoresist, which eliminates parasitic currents and protects the junction from the environment.

The processing of molecular junctions of large area with diameters of 10–100 μm is schematically depicted in Fig. 1 (see Supplementary Information for details). On a 4-inch silicon wafer with a thermally grown oxide, a 1 nm chromium adhesion layer and a 40 nm gold bottom contact are vapour-deposited (Fig. 1a) with a typical root-mean-square roughness of about 0.5 nm for a 1 μm^2 area (see Supplementary Information). Photoresist is spin-coated and holes

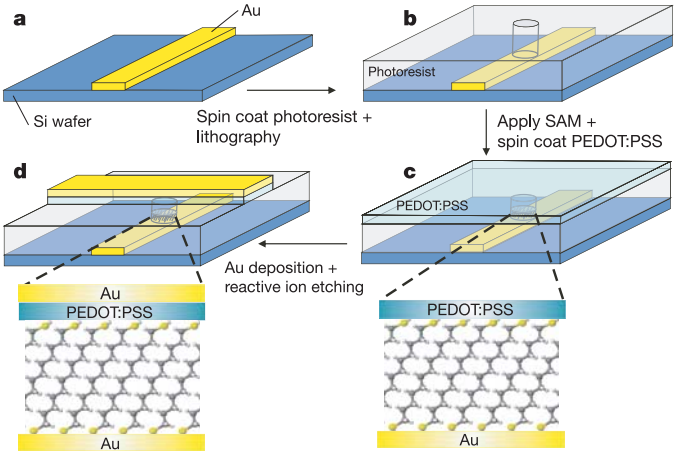

Figure 1 | Processing steps of a large-area molecular junction. a, Gold electrodes are vapour-deposited on a silicon wafer and a photoresist is spin-coated. **b**, Holes are photolithographically defined in the photoresist. **c**, An alkane dithiol SAM is sandwiched between a gold bottom electrode and the highly conductive polymer PEDOT:PSS as a top electrode. **d**, The junction is completed by vapour-deposition of gold through a shadow mask, which acts as a self-aligned etching mask during reactive ion etching of the PEDOT:PSS. The dimensions for these large-area molecular diodes range from 10 to 100 μm in diameter.

[1]Materials Science Centre[Plus], University of Groningen, Nijenborgh 4, NL-9747 AG, Groningen, The Netherlands. [2]Philips Research Laboratories, High Tech Campus 4, NL-5656 AA, Eindhoven, The Netherlands.

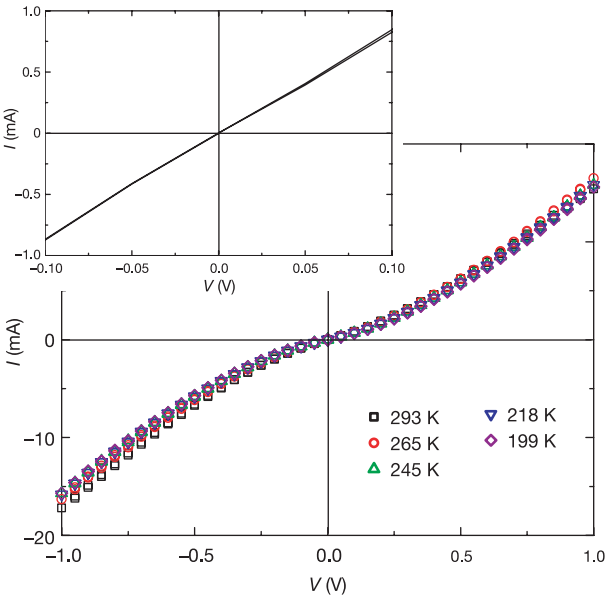

Figure 2 | *I–V* measurements at various temperatures of decanedithiol SAM on a device of diameter 100 μm. The *I–V* characteristics are temperature independent (199–293 K), showing tunnelling as the dominant transport mechanism. Up and down scans are plotted and no hysteresis is observed. Inset, at low bias, a linear *I–V* relationship is obtained, as expected for tunnel junctions.

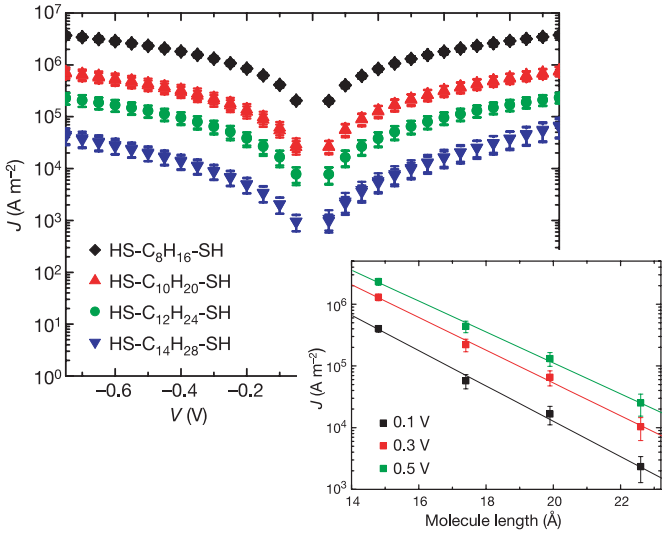

Figure 3 | The current density versus applied voltage for 1,8-octanedithiol, 1,10-decanedithiol, 1,12-dodecanedithiol and 1,14-tetradecanedithiol. The error bars give the standard deviation upon averaging over at least 17 devices. Both up and down scans are plotted. Inset, *J* (on a log scale) at 0.1, 0.3 and 0.5 V bias as a function of the molecular length. This indicates that the transport is by through-bond tunnelling.

of diameter 10–100 μm are produced by standard photolithography (Fig. 1b). The substrate is submerged in a freshly prepared 3×10^{-3} M solution of the alkane dithiol in ethanol for a minimum of 36 h. After the self-assembly of the alkane dithiolate on the gold bottom electrode, a water-based suspension of poly(3,4-ethylenedioxythiophene) stabilized with poly(4-styrenesulphonic acid) (PEDOT:PSS) is spin-coated on top of the SAM, resulting in a layer thickness of about 90 nm (Fig. 1c). PEDOT:PSS is a commercially available, highly doped, conductive polymer with a conductivity of about 30 S cm^{-1}. Next, the top gold electrode is vapour-deposited through a shadow mask. The top electrode acts as a self-aligned etching mask during the removal of the exposed PEDOT:PSS using reactive ion etching (Fig. 1d and Supplementary Information). The yield of functional molecular junctions is over 95%. Here we focus on SAMs of alkane dithiols. SAMs of alkane monothiols are more difficult to use in the processing of hydrophilic PEDOT:PSS owing to their hydrophobic CH_3 end groups. The monothiol-based molecular junctions, however, exhibit similar current versus applied voltage (*I–V*) characteristics, although with a larger standard deviation.

All *I–V* measurements were performed in vacuum to avoid the influence of water in PEDOT:PSS (see Supplementary Information). The *I–V* characteristic of a typical metal–insulator–metal junction 100 μm in diameter and based on decanedithiol is presented in Fig. 2. The current is dominated by the alkane dithiol monolayer. The current in junctions without the SAM is orders of magnitude larger. Figure 2 shows that at low bias the current increases linearly with applied bias (the low bias range is magnified in the inset of Fig. 2). This is expected for a metal–insulator–metal junction when the mean tunnel barrier height is larger than the applied voltage[23]. Similarly, Fig. 2 shows the expected behaviour for a metal–insulator–metal junction at high bias, namely a current that increases exponentially with applied voltage[23]. Furthermore, tunnelling is a temperature-independent process. The absence of any temperature dependence over the range from 199 to 293 K demonstrates that non-resonant tunnelling is the dominant transport mechanism[8] (Fig. 2).

This conclusion is further substantiated by the dependence of the current density on the barrier width. For molecular tunnel junctions, through-bond tunnelling is assumed (ref. 5 and references therein), which implies that the electrons do not tunnel through vacuum but through the lowest unoccupied molecular orbital (LUMO). This is because the mean tunnel barrier height from the Fermi level of the metal to the LUMO is smaller than the work function of the metal. For through-bond tunnelling the width of the tunnel barrier is then equal to the length of the molecule. In Fig. 3 the current density is plotted on a logarithmic scale as a function of the applied voltage for various alkane dithiols: octanedithiol (HS–C_8H_{16}–SH), decanedithiol (HS–$C_{10}H_{20}$–SH), dodecanedithiol (HS–$C_{12}H_{24}$–SH) and tetradecanedithiol (HS–$C_{14}H_{28}$–SH). The synthesis of these alkanedithiols is described in the Supplementary Information. No hysteresis is observed in the *J–V* characteristics during all the voltage sweeps. The error bars represent the standard deviation upon averaging over at least 17 devices. Figure 3 demonstrates that the current density decreases with increased length of the alkane dithiol molecule.

The current density at a bias of 0.1, 0.3 and 0.5 V is presented in the inset of Fig. 3 on a logarithmic scale as a function of the length of the molecule. Molecular lengths were calculated using ACD Labs software (see the Supplementary Information), and the linear fit through the data shows that *J* depends exponentially on the length of the alkane dithiols. This confirms that the currents are indeed specific for the molecules in the junctions. Furthermore, it demonstrates that non-resonant, through-bond tunnelling is the transport mechanism in these metal–insulator–metal junctions. Because current density $J \propto \exp(-\beta d)$ (where d is the barrier width; ref. 23), the tunnelling decay coefficient β can be deduced from the slope of this linear fit. We find β values of 0.66 ± 0.06, 0.61 ± 0.05, and 0.57 ± 0.05 Å^{-1} at a bias of 0.1, 0.3 and 0.5 V, respectively. These values are in good agreement with those derived from analysis of the nanopore diodes by Wang *et al.*, who report values of β ranging from 0.83 to 0.72 Å^{-1} in the bias range from 0.1 to 1.0 V (ref. 8). The decrease of β with increasing bias is also as expected (ref. 5 and references therein). That the current density of our large-area molecular junctions exhibits a dependence on voltage and temperature identical to that of the nanopore devices, combined with the absence of any hysteresis, clearly demonstrates that PEDOT:PSS can be regarded as a non-interacting conductive electrode.

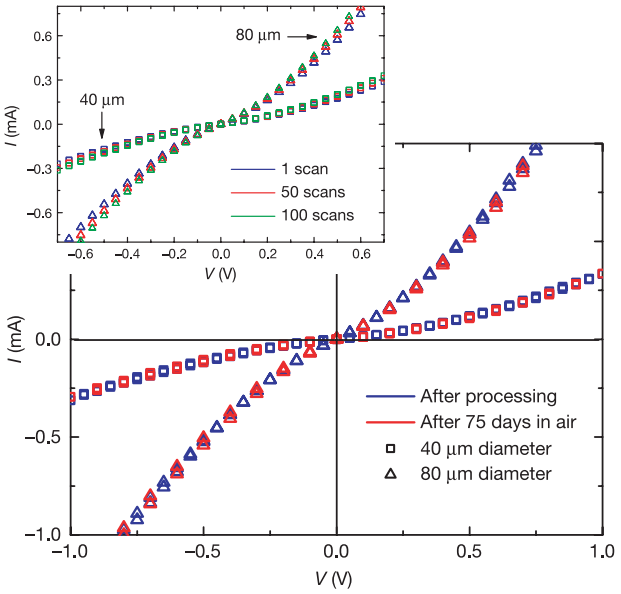

Figure 4 | Stability and operational lifetime of molecular junctions. *I–V* characteristics of molecular junctions based on dodecane dithiol with diameters of 40 μm (squares) and 80 μm (triangles) measured both directly after processing (blue) and after storing under ambient conditions for 75 days (red). Identical *I–V* responses are obtained, which demonstrates the excellent stability of these molecular junctions. The inset shows three *I–V* measurements out of 100 consecutive sweeps of a molecular junction stored under ambient conditions for 75 days with diameters of 40 μm (squares) and 80 μm (triangles). No sign of hysteresis is observed.

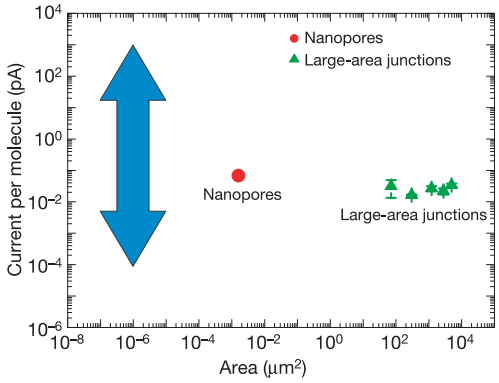

Figure 5 | Current normalized per single molecule for decane(di)thiols at 0.2 V bias versus the device area. Our large-area molecular junctions are presented by the green triangles. Error bars present the standard deviation. Values of current per molecule from the benchmark nanopore junctions are presented by the red circle. Perfect agreement is obtained despite a difference in device area of seven orders of magnitude. The blue arrow presents the intrinsically large scatter in current per molecule obtained from conducting probe atomic force microscopy and scanning tunnelling microscopy measurements.

For practical applications of molecular tunnel junctions, yield, reliability, operational stability and shelf-life are crucial. The yield of functional devices is larger than 95% even for molecular junctions with a diameter of 100 μm. The yield is presumably due to the large differences in surface tension between the hydrophilic PEDOT:PSS and the hydrophobic backbone of the alkane thiolates. This difference prevents intermixing and hence the formation of shorts. The reproducibility is remarkable and investigations into the junction stability are also promising. Figure 4 displays the current–voltage characteristics of molecular junctions based on dodecane dithiol with diameters of 40 μm and 80 μm both directly after fabrication and after storage under ambient conditions for 75 days. The data points fall on top of each other, showing that there is no sign of deterioration upon storage. The inset of Fig. 4 shows three *I–V* measurements taken from 100 consecutive forward and backward sweeps. No hysteresis is observed and there are no differences between consecutive sweeps. The excellent stability is presumably due to encapsulation of the diodes by photoresist, which prevents any interaction of the environment with the SAM.

To compare our molecular junctions to other data appearing in the literature[5,8,12], we normalized the current to the current per single molecule. A grafting density for alkanethiols[5,20] of $4.6 \times 10^{18}\ m^{-2}$ was assumed. As a typical example we use our data for dodecanedithiol. The current per molecule at 0.2 V bias is plotted in Fig. 5 as a function of device area. Literature data are included for measurements on decanethiol in nanopore junctions and by scanning probe experiments, which covers a device area spanning ten orders of magnitude. Figure 5 shows good agreement between our data and the nanopore data[8], with a difference in current per molecule of less than a factor of two. This difference is presumably due to the use of a monothiol in the nanopore junctions and a dithiol in our large-area molecular junctions. Hence, the tunnel barrier width in the nanopore experiments is slightly smaller, resulting in a higher current per molecule. The large scatter in the conducting probe and tunnelling microscope data is intrinsic and due to the presence of an additional tunnelling gap and uncertainties in the number of molecules measured. The good agreement between the current per molecule as measured in our large-area diodes and the nanopore junctions is remarkable considering the orders-of-magnitude difference in device area. In the nanopore junctions the current is measured through molecules that are perfectly ordered in a mono-domain, while in the large-area diodes the molecules are ordered in multi-domains. Grain boundaries in SAMs do not seem to impede charge transport.

In summary, we have demonstrated a technique for fabricating reliable molecular metal–insulator–metal junctions with unprecedented device diameters of up to 100 μm. The yield of these molecular junctions is close to 100%. Preliminary stability investigations reveal a shelf life of more than several months and no deterioration upon cycling. The current per molecule is similar to that obtained for benchmark nanopore diodes. Key ingredients are the use of a conducting polymer layer sandwiched between the SAM and the top electrode to prevent electrical shorts, and processing within lithographically defined vertical interconnects (or via holes) to prevent both parasitic currents and interaction between the environment and the SAM. The technique is simple, compatible with standard integrated circuit fabrication processes, and can be scaled up and extended to any molecule and any metal bottom electrode on which an ordered SAM can be formed.

Received 6 September 2005; accepted 2 March 2006.

1. Reed, M. A., Zhou, C., Muller, C. J., Burgin, T. P. & Tour, J. M. Conductance of a molecular junction. *Science* **278,** 252–254 (1997).
2. Joachim, C., Gimzewski, J. K. & Aviram, A. Electronics using hybrid-molecular and mono-molecular devices. *Nature* **408,** 541–548 (2000).
3. Nitzan, A. & Ratner, M. A. Electron transport in molecular wire junctions. *Science* **300,** 1384–1389 (2003).
4. Aviram, A. & Ratner, M. A. Molecular rectifiers. *Chem. Phys. Lett.* **29,** 277–283 (1974).
5. Salomon, A. *et al.* Comparison of electronic transport measurements on organic molecules. *Adv. Mater.* **15,** 1881–1890 (2003).
6. Szuchmacher Blum, A. *et al.* Molecularly inherent voltage-controlled conductance switching. *Nature Mater.* **4,** 167–172 (2005).
7. Collier, C. P. *et al.* Electronically configurable molecular-based logic gates. *Science* **285,** 391–394 (1999).
8. Wang, W., Lee, T. & Reed, M. A. Mechanism of electron conduction in self-assembled alkanethiol monolayer devices. *Phys. Rev. B* **68,** 035416 (2003).
9. Zhitenev, N. B., Meng, H. & Bao, Z. Conductance of small molecular junctions. *Phys. Rev. Lett.* **88,** 226801 (2002).
10. Chen, Y. *et al.* Nanoscale molecular-switch crossbar circuits. *Nanotechnology* **14,** 462–468 (2003).
11. Cui, X. D. *et al.* Reproducible measurements of single-molecule conductivity. *Science* **294,** 571–574 (2001).

12. Engelkes, V. B. *et al.* Length-dependent transport in molecular junctions based on SAMs of alkanethiols and alkanedithiols: Effect of metal work function and applied bias on tunneling efficiency and contact resistance. *J. Am. Chem. Soc.* **126,** 14287–14296 (2004).
13. Reichert, J. *et al.* Driving current through single organic molecules. *Phys. Rev. Lett.* **88,** 176804 (2002).
14. Smit, R. H. M. *et al.* Measurement of the conductance of a hydrogen molecule. *Nature* **419,** 906–909 (2002).
15. Zhou, C. *et al.* Nanoscale metal/self-assembled monolayer/metal heterostructures. *Appl. Phys. Lett.* **71,** 611–613 (1997).
16. de Boer, B. *et al.* Metallic contact formation for molecular electronics: Interactions between vapor-deposited metals and self-assembled monolayers of conjugated mono- and dithiols. *Langmuir* **20,** 1539–1542 (2004).
17. Haick, H., Ghabboun, J. & Cahen, D. Pd versus Au as evaporated metal contacts to molecules. *Appl. Phys. Lett.* **86,** 042113 (2005).
18. Haynie, B. C. *et al.* Adventures in molecular electronics: how to attach wires to molecules. *Appl. Surf. Sci.* **203/204,** 433–436 (2003).
19. de Boer, B. *et al.* Synthesis and characterization of conjugated mono- and dithiol oligomers and characterization of their self-assembled monolayers. *Langmuir* **19,** 4272–4284 (2003).
20. Love, J. C. *et al.* Self-assembled monolayers of thiolates on metals as a form of nanotechnology. *Chem. Rev.* **105,** 1103–1169 (2005).
21. Porter, M. D. *et al.* Spontaneously organized molecular assemblies. 4. Structural characterization of *n*-alkyl thiol monolayers on gold by optical ellipsometry, infrared spectroscopy, and electrochemistry. *J. Am. Chem. Soc.* **109,** 3559–3568 (1987).
22. Chang, S.-C. *et al.* Investigation of a model molecular-electronic rectifier with an evaporated Ti-metal top contact. *Appl. Phys. Lett.* **83,** 3198–3200 (2003).
23. Simmons, J. G. Generalized formula for the electric tunnel effect between similar electrodes separated by a thin insulating film. *J. Appl. Phys.* **34,** 1793–1803 (1963).

Supplementary Information is linked to the online version of the paper at www.nature.com/nature.

Acknowledgements We thank M. Mulder, T. C. T. Geuns, E. A. Meulenkamp, E. Cantatore and S. Bakker for their assistance, and the Materials Science Centre^{Plus} for financial support.

Author Information Reprints and permissions information is available at npg.nature.com/reprintsandpermissions. The authors declare no competing financial interests. Correspondence and requests for materials should be addressed to B.d.B. (b.de.boer@rug.nl).